



HAL
open science

A PEDOT-Pt-TiO₂ hybrid material synthesized by the casting method for photocatalytic hydrogen generation

Marek Kobylański, Agnieszka Tercjak, Hynd Remita, Xiaojiao Yuan, Onur Cavdar, Junkal Gutierrez, Adriana Zaleska-Medynska

► To cite this version:

Marek Kobylański, Agnieszka Tercjak, Hynd Remita, Xiaojiao Yuan, Onur Cavdar, et al.. A PEDOT-Pt-TiO₂ hybrid material synthesized by the casting method for photocatalytic hydrogen generation. *Advances in Natural Sciences: Nanoscience and Nanotechnology*, 2023, 14 (4), pp.045017. 10.1088/2043-6262/ad095c . hal-04347866

HAL Id: hal-04347866

<https://hal.science/hal-04347866>

Submitted on 15 Dec 2023

HAL is a multi-disciplinary open access archive for the deposit and dissemination of scientific research documents, whether they are published or not. The documents may come from teaching and research institutions in France or abroad, or from public or private research centers.

L'archive ouverte pluridisciplinaire **HAL**, est destinée au dépôt et à la diffusion de documents scientifiques de niveau recherche, publiés ou non, émanant des établissements d'enseignement et de recherche français ou étrangers, des laboratoires publics ou privés.

A PEDOT-Pt-TiO₂ hybrid material synthesized by the casting method for photocatalytic hydrogen generation

Marek P. Kobylański¹, Agnieszka Tercjak², Hynd Remita³, Xiajiao Yuan^{3,4}, Onur Cavdar¹, Junkal Gutierrez², Adriana Zaleska-Medynska¹

¹ Department of Environmental Technology, Faculty of Chemistry, University of Gdansk, Wita Stwosza str 63, 80-308 Gdansk, Poland

² Group 'Materials + Technologies', Department of Chemical and Environmental Engineering, Faculty of Engineering Gipuzkoa, University of the Basque Country (UPV/EHU), Plaza Europa 1, 20018 Donostia-San Sebastián, Spain

³ Institut de Chimie Physique, UMR 8000 CNRS, Université Paris-Saclay, 91405 Orsay, France

⁴ Institut Català d'Investigació Química 16, Avinguda dels Països Catalans, 43007 Tarragona

Abstract

This study describes the synthesis and characterization of a hybrid material consisting of titanium dioxide nanotube arrays (TiO₂ NTs) modified by platinum nanoparticles (Pt-TiO₂ NTs) *via* radiolysis and a conductive poly(3,4-ethylenedioxythiophene) (PEDOT) layer, for the first time. The NTs were fabricated by a two-step anodic oxidation process and exhibited different morphologies using electrolyte solutions with different water contents (2–10 vol%). The polymer layer of poly(3,4-ethylenedioxythiophene)-poly(styrenesulfonate) (PEDOT:PSS) was coated on the Pt-TiO₂ scaffold using the casting method. The PEDOT:PSS-Pt-TiO₂ NTs exhibited stability in the photocatalytic process after additional calcination; the nanotubes with lengths of ~3 μm exhibited the highest photocatalytic activity (~4.5x10⁻³ μmol·cm⁻² of H₂). Additionally, the samples obtained from electrolyte solutions containing 5 and 10 vol% water exhibited nanostructures with the highest catalytic activity.

Keywords: Hybrid nanomaterials, Titanium dioxide nanotube arrays, Radiolysis, The casting method, Hydrogen-photogeneration catalysis

1. Introduction

Composites containing semiconductors and polymers have been extensively investigated in the last 10 years due to their unique properties. Polymeric materials enhance the optical, conductive, and photocatalytic properties of nanotubes [1,2], forming materials with high surface areas, good conductivity [3,4], and biocompatibility [5]. TiO₂ nanotubes (TiO₂ NTs) are nanotubular structures that are commonly modified by polymeric materials [6]. They have been utilized in medicine [7], water and air treatment [8], electronic devices [9,10], lithium-ion batteries [11–13], sensors [14,15], and solar cells [16–18].

Numerous investigations have focused on using nanoparticles to enhance the properties of polymers [19–23]. However, the ability of polymers to intensify the features of nanomaterial scaffolds using a semiconductor still requires investigation. Hence, this study aimed to synthesize and analyze the properties of a polymer-modified inorganic nanomaterial. Synthesizing nanoparticles using a polymer-material-embedded matrix is a major challenge. Moreover, the synthetic strategy used to fabricate NT-polymers hybrid materials determine the morphology and properties of the new material. Thus, the matrix, its morphology, and potential applications should be considered while selecting the modification route [1].

Hierarchical TiO₂ NTs obtained *via* anodic oxidation are used as scaffolds for polymeric materials [18, 24–26]. Electropolymerization is commonly used to synthesize hybrid materials composed of TiO₂ NTs and polymers [12,13,24–29]; This synthetic route enables the fabrication of conductive polymer layers using monomers coupled to an electrode surface. The growth rate and thickness of the polymer layer can be controlled by the current density, applied voltage, and charge values [30]. However, the practicability of this method is limited

due to scaling-up difficulties [1]. Hybrid materials containing polymer-modified TiO₂ NTs are also fabricated *via* casting, spin-coating and dip-coating [1,16,17]; these methods utilize matrix and polymer solutions, making them easily retrievable. Surprisingly, very few studies have utilized these methods to synthesize hybrid materials.

Therefore, this study aimed to fabricate and characterize photoactive hybrid materials containing TiO₂ NTs and a conductive polymer (PEDOT). Platinum particles were deposited on the surface of the TiO₂ NTs *via* radiolysis to improve the photocatalytic properties of the composites [31]. Additionally, the effects of the morphology and synthetic route of the TiO₂-NT matrix on the hybrid material were analyzed to optimize the conditions for the fabrication of Pt-polymer-TiO₂-NT hybrid materials for the model reaction of hydrogen photogeneration.

2. Material and Methods

2.1. TiO₂ NT fabrication

Titanium foil (Sigma Aldrich) was cut into pieces (3 cm x 2 cm), cleaned using ultrasound for 10 min in acetone, isopropanol, methanol, and deionized water, and subsequently dried in a stream of air. A cylindrical platinum mesh was used as the counter electrode. The process was carried out at room temperature for 60 min at 40 V using a solution of ammonium fluoride (0.09 M) in a mixture of ethylene glycol and deionized water (90–98 and 2–10% v/v, respectively) as the electrolyte. Anodic oxidation was carried out under 40 V at room temperature using a MANSION SDP 2603 power supply. After anodic oxidation, the NTs were completely removed from the surface using an ultrasonic bath, followed by another anodic oxidation. Subsequently, the samples were dried for 24 h at 80 °C and calcined at 450 °C for 1 h using a temperature gradient of 2 °C/min.

2.2. Radiodeposition of platinum particles on the NT surface

Platinum particles were deposited on the surface of the NTs *via* radiolysis. The determination of the amount of Pt precursor to be used to enable the photocatalytic application of the fabricated materials has been described in the Supporting Materials. After applying 150 µl of a 0.1 M solution of Pt(acac) (Sigma Aldrich) in isopropanol (Sigma Aldrich) on the TiO₂-nanotube surface, the samples were placed in a Petri dish, and the platinum ions were reduced by γ -irradiation (2.5 kGy·h⁻¹) under a nitrogen atmosphere. Radioreduction, using ⁶⁰Co as the source of γ radiation, was continued for 6 h. Radiolysis is a powerful technique to synthesize

metal nanoparticles of controlled size, shape and structure in solutions and on supports [32, 33] . The metal complexes are reduced by solvated electrons and radicals (here alcohol radicals) induced by solvent radiolysis.

2.3. Casting of the polymer layer

The samples were modified with the PEDOT: PSS layer, which was cast directly on the surface of the Pt-TiO₂ nanotubes. One drop of the PEDOT: PSS solution was applied on the surface of the matrix, and some samples were additionally heated at 350 °C for 1 h to remove the PSS. Furthermore, the most suitable method for polymer casting on the NT surface was determined (it has been described in the Supporting Materials).

2.4. Surface properties

Scanning electron microscope (SEM) images of the surface of analyzed hybrid materials were collected in a Hitachi S-4800 with an accelerating voltage of 5 kV.

X-ray diffraction (XRD) was performed on a Philips PW 1710 diffractometer. The Cu K α X-ray source was set to 40 kV and 100 mA and the hybrid materials were examined at room temperature in the angular range of 10° to 30°.

The elemental compositions of hybrid materials were analyzed by X-ray Photoelectron Spectroscopy (XPS, SPECS). The XPS was equipped with a Phoibos 150 1D-DLD energy analyzer-with Al K monochromatic radiation ($h\nu = 1486.7$ eV).

The optical properties of the materials were analyzed using a UV 2600 spectrophotometer (Shimadzu) with a barium sulfate integrating sphere attachment as a reference sample. The spectra were recorded in the wavelength range of 300–700 nm.

To estimate the recombination rate of the reactive electron-hole pairs, luminescence spectra of the samples were recorded by an LS-50B luminescence spectrometer (Perkin Elmer) using an excitation wavelength of 300 nm.

Fourier transform infrared spectroscopy (FTIR) spectra were done using a Nicolet Nexus Spectra equipped with a Golden Gate single reflection diamond ATR accessory. The FTIR spectra of hybrid materials were taken with a 2 cm^{-1} resolution in a wavenumber range from 4000 to 400 cm^{-1} .

A semiconductor characterization system (Keithley model 4200-SCS) was used to study the conductive properties of the hybrid materials. Two-point probe experiments were carried out applying current from X to Y V to verify the response of the investigated hybrid materials.

2.5. Photocatalytic hydrogen generation

Unmodified and modified TiO_2 nanotubes were placed in a Teflon reactor (equipped with quartz glass and a cooling system) with a reactor volume of 30 cm^3 . For hydrogen photogeneration, 20 mL of an aqueous solution containing 5 wt% methanol was used at a temperature of $20\text{ }^\circ\text{C}$. An Oriel 1000-W Xe lamp was used as the light source with an irradiation intensity of 100 mW/cm^2 . After placing the sample in the reactor, the reaction space was filled with the methanol solution. Subsequently, the system was purged with nitrogen for air removal and an equilibrium state was attained by constantly stirring the solution at 500 rpm for 30 min. Samples ($200\text{ }\mu\text{L}$) were collected each hour; The hydrogen content was determined by gas chromatography-thermal conductivity detector (GC-TCD) using a calibration curve. The preparation of the calibration curve has been described in the Supporting Materials.

3. Results

3.1. Morphology

Fig. 1 shows the synthesis and modification scheme of the TiO₂ NTs. The samples exhibited different NT morphology, controlled by the water content of the electrolyte used during anodic oxidation (in the range of 2–10% v/v) and the nanotube-layer modification steps. NT modification involved deposition of platinum nanoparticles by radiolysis, PEDOT:PSS layer casting, and the thermal decomposition of PSS. This process was used to analyze the influence of the matrix morphology and its modification on the properties of the hybrid material.

Scanning electron microscopy was used to analyze the surface structure of the synthesized material. As a multistep synthetic procedure was used, the morphology was analyzed after each modification step (Fig. 2). The synthesized NTs exhibited lengths in the range of 2.10–6.60 μm, consistent with previous reports of nanostructures obtained under similar conditions [34]; the samples obtained using electrolyte solutions containing 5 and 10 vol% water exhibited comparable NT lengths (~3 μm). The synthesized NTs exhibited internal and external diameters in the range of 107–140 nm and 37–85 nm, respectively. Increasing the water content of the electrolyte solution during anodic oxidation increased the external and internal diameters, and the space between the individual nanotubes, thus, increasing the water content decreased the active surface of the hybrid material [35, 36].

Additionally, the space between the nanotubes facilitated the deposition of polymeric material on the walls and deep penetration of the NTs into the scaffold. The diameter dimensions of the PEDOT-Pt-TiO₂_5% sample could not be accurately defined because the polymer layer filled the spaces between the nanotubes forming a core-sheath structure. The structure did not exhibit any changes on annealing (to thermally degrade PSS from the polymer layer), and no significant differences were observed in the recorded photos after calcination at 350 °C.

Notably, the morphology of the Pt-TiO₂_5% sample singularized after modification by the PEDOT: PSS layer; the polymer layer filled the spaces between the NTs, coating each nanotube. Its morphology remained unchanged after the thermal decomposition of PSS through calcination. The core-shell structure prevented the unequivocal determination of the NT diameter size for PEDOT:PSS-Pt-TiO₂_5% and PEDOT-Pt-TiO₂_5%.

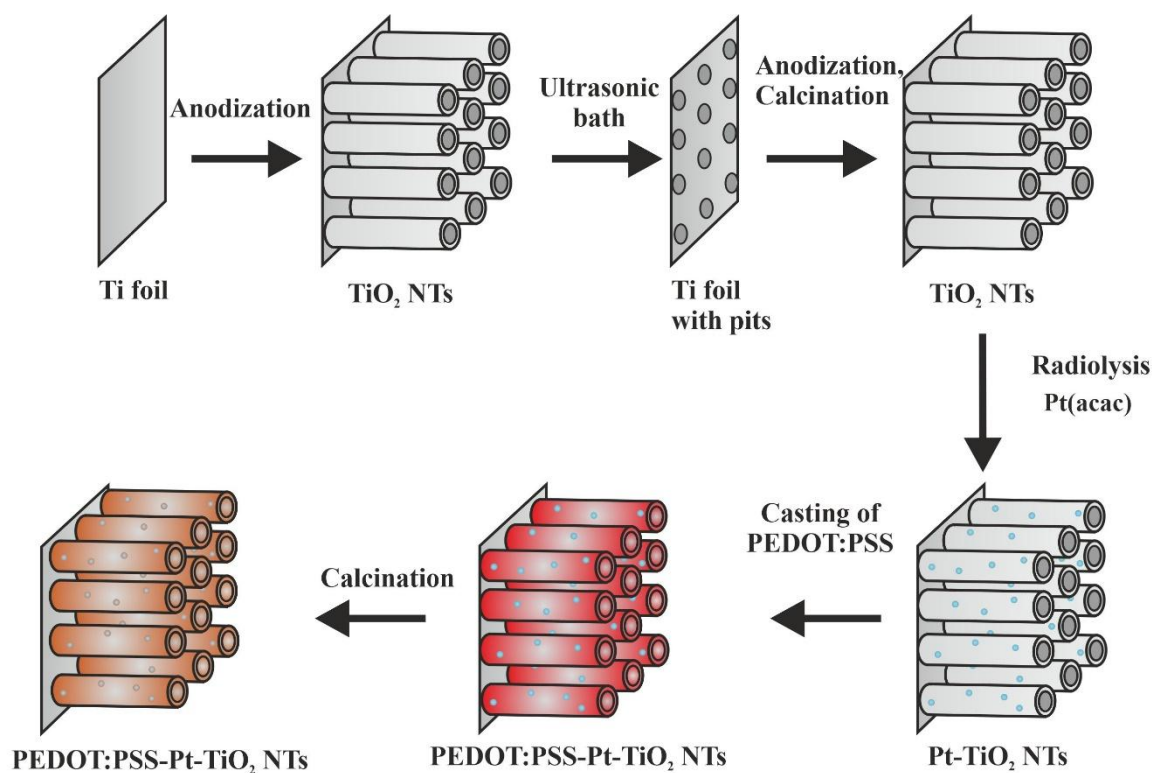


Fig. 1. The manufacture of PEDOT-Pt-TiO₂ NTs (showing the intermediate stages).

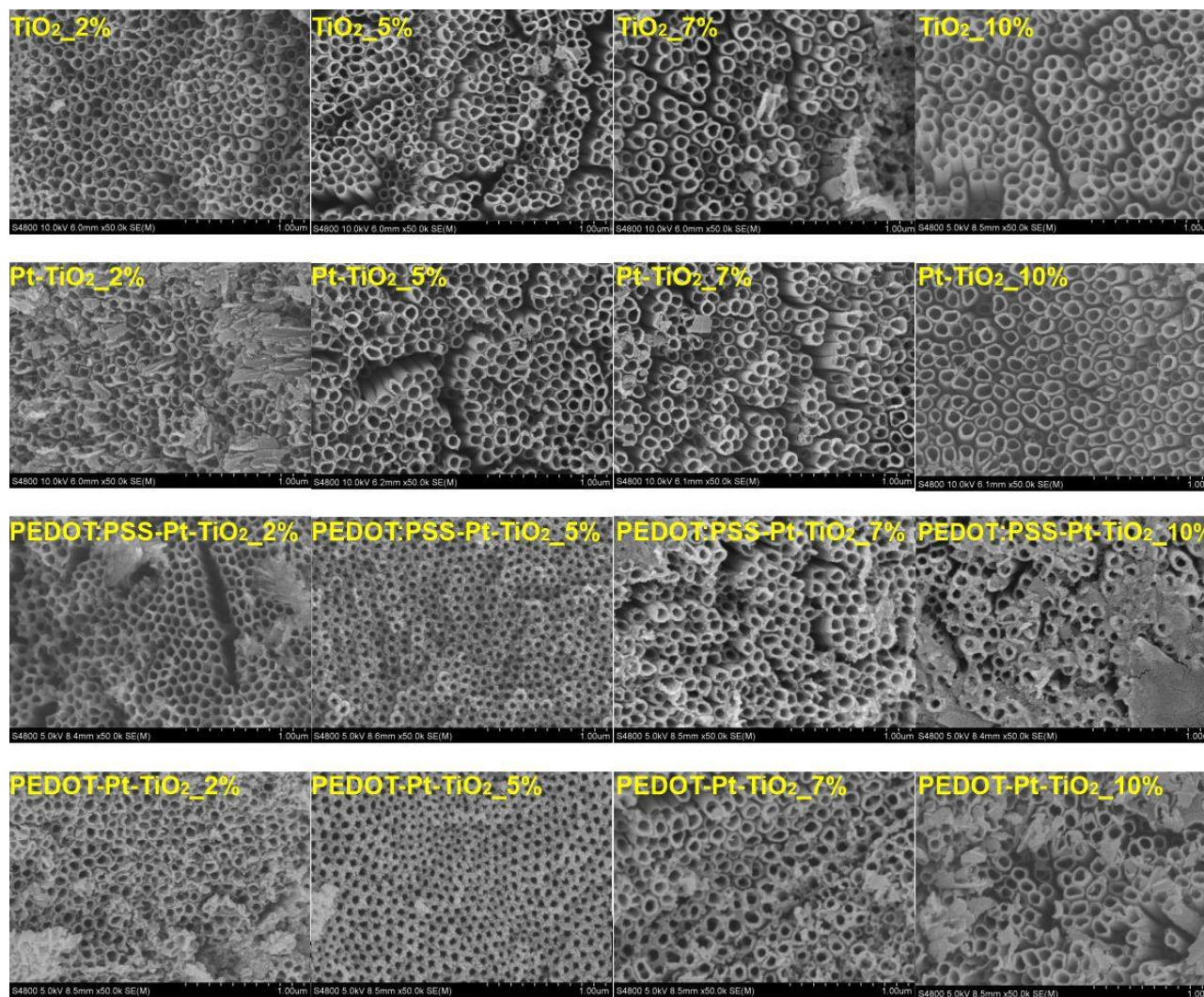


Fig. 2. Morphology of TiO_2 NTs fabricated using electrolyte solutions containing different amounts of water (horizontal); their surfaces after each modification step (vertical).

Table 1. Morphology of the TiO₂ NTs before and after each modification step

Sample label	Preparation	Length	Inner diameter	External diameter
		(μm)	(nm)	(nm)
TiO ₂ _2%	2-step anodization, calcination at 450 °C	6.50 ± 0.2	107 ± 10	37 ± 5
TiO ₂ _5%		3.10 ± 0.1	113 ± 12	71 ± 1
TiO ₂ _7%		2.10 ± 0.1	120 ± 8	78 ± 2
TiO ₂ _10%		3.15 ± 0.2	127 ± 7	79 ± 3
Pt-TiO ₂ _2%	2-step anodization, calcination at 450 °C, radioreduction of Pt	6.35 ± 0.2	106 ± 8	40 ± 4
Pt-TiO ₂ _5%		3.25 ± 0.1	108 ± 9	73 ± 2
Pt-TiO ₂ _7%		2.10 ± 0.1	119 ± 8	75 ± 3
Pt-TiO ₂ _10%		3.30 ± 0.2	125 ± 5	81 ± 4
PEDOT:PSS-Pt-TiO ₂ _2%	2-step anodization, calcination at 450 °C, radioreduction of Pt, PEDOT: PSS casting	6.60 ± 0.1	111 ± 13	71 ± 8
PEDOT:PSS-Pt-TiO ₂ _5%		3.00 ± 0.1	115 ± 8	75 ± 7
PEDOT:PSS-Pt-TiO ₂ _7%		2.15 ± 0.2	130 ± 10	65 ± 8
PEDOT:PSS-Pt-TiO ₂ _10%		3.20 ± 0.3	120 ± 8	73 ± 7
PEDOT-Pt-TiO ₂ _2%	2-step anodization, calcination at 450 °C, radioreduction of Pt, PEDOT: PSS casting, calcination at 350 °C	6.20 ± 0.2	104 ± 8	63 ± 9
PEDOT-Pt-TiO ₂ _5%		3.20 ± 0.3	----	55 ± 7
PEDOT-Pt-TiO ₂ _7%		2.30 ± 0.2	147 ± 20	63 ± 9
PEDOT-Pt-TiO ₂ _10%		3.50 ± 0.3	140 ± 17	85 ± 11

3.2. Surface properties

XRD patterns were recorded for the Pt-TiO₂ samples fabricated using electrolytes containing different amounts of water (Fig. 3(a)); additionally, a PEDOT-Pt-TiO₂_2% analysis was carried out after each modification step (Fig. 3(b)). All the diffractograms exhibited signals characteristic to anatase at $2\theta = 25^\circ$ and titanium form (Ti foil) at $2\theta = 40^\circ$ [37]. The samples fabricated using electrolytes with different water contents exhibited similar results. The diffractogram of the NTs modified by PEDOT: PSS exhibited a wide signal in the range of $2\theta = 15\text{--}35^\circ$ due to the presence of PEDOT: PSS on the NT surface [38].

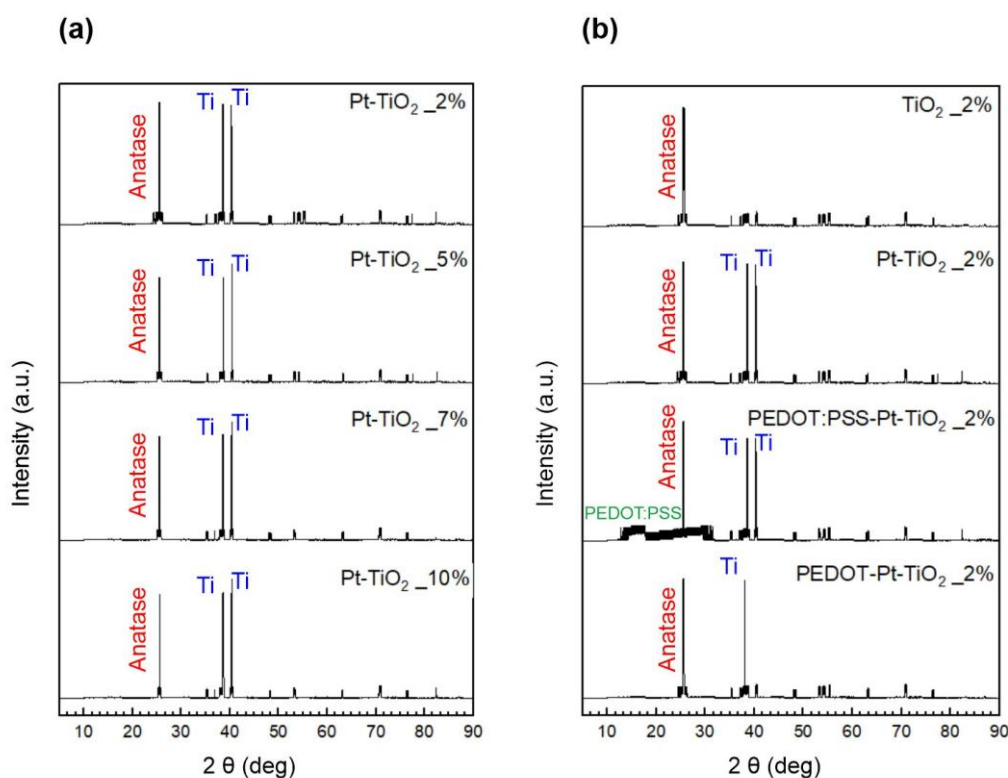


Fig. 3. XRD patterns for samples obtained: (a) Using electrolyte solutions containing different amounts of water, (b) After each fabrication step.

XPS analysis was used to determine the elemental composition of the samples after platinum radioreduction (Table S2). Although oxygen, titanium, nitrogen, and carbon were detected on the surface of each sample, the presence of platinum could not be confirmed by

the XPS analysis. This is possibly because XPS analyzes a small area of the sample. It is possible that platinum nanoparticles are deposited inside the sample [35, [39].

Subsequently, attenuated total reflectance-fourier transform infrared (ATR-FTIR) spectroscopy was used to characterize the samples further (Fig. S2-). Signals were observed in the range of 1250–1100 cm^{-1} due to the SO^{3-} group of PSS [40]. The thermal degradation of PSS was confirmed by a lack of the SO^{3-} signals in the samples annealed at 350 °C (marked as PEDOT) and the presence of peaks attributed to C-O-C (1250 cm^{-1}) and C=C bonds (1600 cm^{-1}) [41]. The unmodified nanotubes exhibited a signal at 500 cm^{-1} due to Ti [41,42]. Notably, all the samples exhibited similar spectra after the same modification step, regardless of the electrolyte composition (*i.e.*, the morphology of the samples).

To confirm the presence of platinum in the NTs, conductivity tests were carried out before and after radiolysis (Fig. S1). The conductivity increased after modification by γ -irradiation; This was attributed to the deposition of platinum particles on the NTs [43].

3.3. Photocatalytic hydrogen generation

The model reaction of photocatalytic hydrogen generation was used to investigate the photocatalytic activity of the TiO_2 NTs modified by the conductive polymer; The results are summarized in Table 3. Materials containing PEDOT: PSS were unstable in aqueous phase; thus, they were not tested in the model reaction.

As shown in Fig. 4, the modification of the TiO_2 NTs with platinum and the conductive polymer increased their hydrogen-generation efficiency. PEDOT-Pt- TiO_2 _10% exhibited the highest photocatalytic activity with $4.5 \times 10^{-3} \mu\text{mol}\cdot\text{cm}^{-2}$ of photogenerated hydrogen after 4 h of irradiation. Similar hydrogen production ($4.3 \times 10^{-3} \mu\text{mol}\cdot\text{cm}^{-2}$ after 4 h of irradiation) was observed using the NTs fabricated in the electrolyte contained 5 vol% water.

The aforementioned photocatalysts exhibited similar NT-layer thickness values (of $\sim 3 \mu\text{m}$); Therefore, a TiO_2 -NT length of $3 \mu\text{m}$ is optimal for the hydrogen generation process. Furthermore, the TiO_2 _2% sample, with the longest nanotubes ($\sim 6 \mu\text{m}$), exhibited the lowest hydrogen-photogeneration activity. Earlier reports indicate that the TiO_2 NTs obtained in electrolytes containing 2 vol% of water exhibit enhanced photocatalytic activity in the model reaction of pollutant photodecomposition [31–33, 41]. Additionally, they indicate that the TiO_2 -NT lengths exhibiting the highest photocatalytic activity for pollutant photodegradation in the water and gas phase cannot be effectively used for hydrogen photogeneration. This is consistent with the results of this study.

Very few publications describe the utilization of TiO_2 NTs for hydrogen photogeneration. The earliest publication describes a photocatalyst (TiO_2 NTs modified by Pt nanoparticles; with NTs exhibiting an inner diameter of 120 nm and length of $10 \mu\text{m}$) with a higher hydrogen-photogeneration efficiency ($25.0 \mu\text{mol h}^{-1}\cdot\text{cm}^{-2}$) than that obtained in this study [45]. Another publication describes a hydrogen photogeneration process utilizing Pt-modified TiO_2 NTs obtained by an anodic oxidation process with a powder-form photocatalyst [46]; This process produces $30 \text{ mmol}\cdot\text{g}^{-1}\cdot\text{h}^{-1}$ of photogenerated hydrogen, which is higher than the efficiency of the photocatalyst in the form of a thin NT film on a Ti plate. However, the separation and reuse of photocatalysts in the powder form from electrolytes is challenging. According to previous publications, nanotubes fabricated by the hydrothermal method exhibit a hydrogen-photogeneration efficiency of $0.27 \mu\text{mol}\cdot\text{min}^{-1}$ [47] and $15.7 \text{ mmol}\cdot\text{g}^{-1}\cdot\text{h}^{-1}$ [48].

This study could not confirm an enhancement in the photocatalytic properties of Pt- TiO_2 on modification with a conductive polymer. Only the Pt- TiO_2 _10% sample exhibited an increase in hydrogen photogeneration after polymer-layer casting; for the remaining samples, hydrogen photogeneration decreased on modification with the polymeric material (Fig. 4).

Table 2. Photocatalytic activities of the TiO₂ nanotubes and hybrid materials (PEDOT- Pt-TiO₂) in the model reaction of hydrogen photogeneration.

Sample label	Amount of hydrogen after 4 h of irradiation ($\mu\text{mol}\cdot\text{cm}^{-2}$)
TiO ₂ _2%	1.84×10^{-4}
TiO ₂ _5%	7.15×10^{-4}
TiO ₂ _7%	3.30×10^{-4}
TiO ₂ _10%	5.11×10^{-5}
Pt-TiO ₂ _2%	6.62×10^{-4}
Pt-TiO ₂ _5%	4.60×10^{-3}
Pt-TiO ₂ _7%	2.75×10^{-3}
Pt-TiO ₂ _10%	3.45×10^{-3}
PEDOT:PSS-Pt-TiO ₂ _2%	Sample unstable in aqueous solution
PEDOT:PSS-Pt-TiO ₂ _5%	Sample unstable in aqueous solution
PEDOT:PSS-Pt-TiO ₂ _7%	Sample unstable in aqueous solution
PEDOT:PSS-Pt-TiO ₂ _10%	Sample unstable in aqueous solution
PEDOT -Pt-TiO ₂ _2%	9.75×10^{-5}
PEDOT -Pt-TiO ₂ _5%	4.33×10^{-3}
PEDOT -Pt-TiO ₂ _7%	1.52×10^{-3}
PEDOT -Pt-TiO ₂ _10%	4.51×10^{-3}

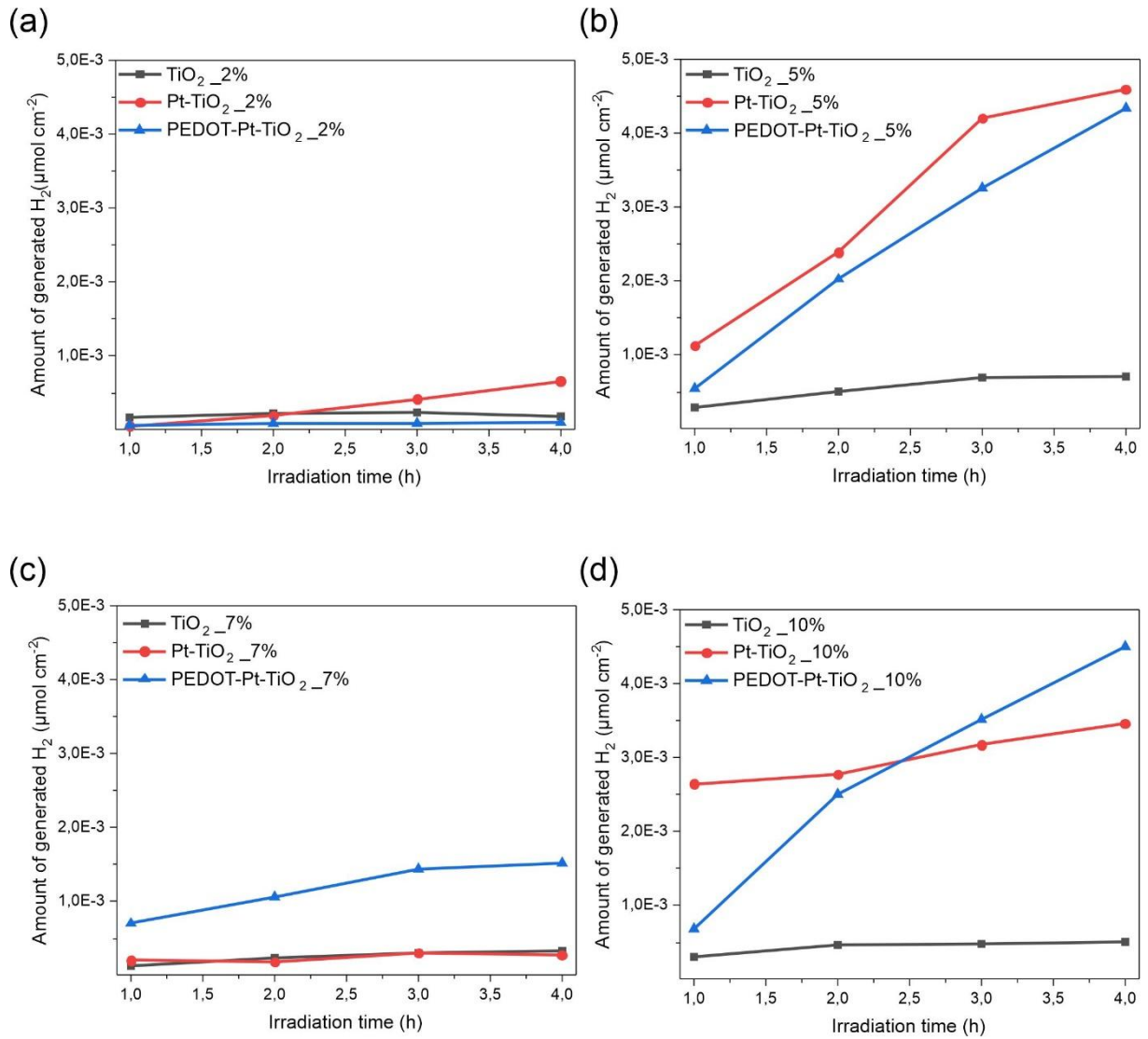


Fig. 4. Photocatalytic activities of the hydrogen photogeneration reaction exhibited by the modified and unmodified TiO₂ NTs obtained in electrolytes containing: a) 2%, b) 5%, c) 7%, and d) 10% water.

4. Conclusions

The multistep modification of TiO₂ NTs with Pt nanoparticles and a conductive polymer increased the photocatalytic activity of the nanomaterial in the model reaction of hydrogen generation. Nanotube scaffolds fabricated in electrolyte solutions containing 5 and 10 vol% water exhibited the highest photocatalytic activities, producing 0.45 μmol·h⁻¹ of photogenerated hydrogen. Increasing the water content of the electrolyte solution influenced the morphology of the fabricated nanotubes. NT scaffolds with a thickness of 3 μm exhibited the highest photoactivity; the space between the nanotubes facilitated a deep penetration of the polymer solution. Although the PEDOT: PSS layer on the TiO₂ NT surface was unstable in the aqueous phase, the annealing of the composite at 350 °C (to remove PSS) increased the stability of the fabricated material.

Authorship Statement

Acknowledgments

This research was funded by the Polish National Science Center, grant number 2017/27/N/ST8/00946.

Declaration of Competing Interest

The authors have no conflicts of interest to declare that are relevant to the content of this article.

References

- [1] S. Abdelnasser, G. Park, H. Han, R. Toth, H. Yoon, Enhanced photocatalytic performance of poly(3,4-ethylenedioxythiophene)-coated TiO₂ nanotube electrodes, *Synth. Met.* 251 (2019) 120–126,

<https://doi.org/10.1016/j.synthmet.2019.03.018>

- [2] L. Yang, Y. Yu, J. Zhang, F. Chen, X. Meng, Y. Qiu, Y. Dan, L. Jiang, In-situ fabrication of diketopyrrolopyrrole-carbazole-based conjugated polymer/TiO₂ heterojunction for enhanced visible light photocatalysis, *Appl. Surf. Sci.* 434 (2018) 796–805, <https://doi.org/10.1016/j.apsusc.2017.10.176>
- [3] F. Wang, X. Zhang, L. Yang, D. Xu, Y. Ma, D. Chen, L. Wang, C. Zhao, W. Yang, A Scalable route to prepare core-shell structured ZnO@PEDOT nanowires and PEDOT nanotubes and their properties as electrode materials, *Appl. Surf. Sci.* 370 (2016) 102–110, <https://doi.org/10.1016/j.apsusc.2016.02.159>
- [4] M. Szkoda, K. Trzcinski, J. Rysz, M. Gazda, K. Siuzdak, A. Lisowska-Oleksiak, Electrodes consisting of PEDOT modified by Prussian Blue analogues deposited onto titania nanotubes – their highly improved capacitance, *Solid State Ion.* 302 (2017) 197–201, <https://doi.org/10.1016/j.ssi.2016.12.025>
- [5] J. H. Huang, T. C. Lai, L. C. Cheng, R. S. Liu, C. H. Lee, M. Hsiao, C. H. Chen, L. J. Her, D. P. Tsai, Modulating cell-uptake behavior of Au-based nanomaterials via quantitative biomolecule modification, *J. Mater. Chem.* 21 (2011) 14821–14829, <https://doi.org/10.1039/C1JM11365H>
- [6] W. A. Abbas, I. H. Abdullah, B. A. Ali, N. Ahmed, A. M. Mohamed, M. Y. Rezk, N. Ismail, M. A. Mohamed, N. K. Allam, Recent advances in the use of TiO₂ nanotube powder in biological, environmental, and energy applications, *Nanoscale Adv.* 1 (2019) 2801–2816, <https://doi.org/10.1039/C9NA00339H>
- [7] C. C. Torres, C. H. Campos, C. Diaz, V. A. Jimenez, F. Vidal, L. Guzman, J. B. Alderete, PAMAM-grafted TiO₂ nanotubes as novel versatile materials for drug delivery applications, *Mater. Sci. Eng. C* 65 (2016) 164–171, <https://doi.org/10.1016/j.msec.2016.03.104>
- [8] Y. Wu, Y. Li, A. Tian, K. Mao, J. Liu, Selective removal of perfluorooctanoic acid using molecularly imprinted polymer-modified TiO₂ nanotube arrays, *Int. J. Photoenergy*, 2016 (2016) e7368795, <https://doi.org/10.1155/2016/7368795>
- [9] N. K. Sidhu, R. R. Thankalekshmi, A. C. Rastogi, Solution processed TiO₂ nanotubular core with polypyrrole conducting polymer shell structures for supercapacitor energy storage devices, *MRS Proceedings*, 1547 (2013) 69–74, <https://doi.org/10.1557/opl.2013.636>
- [10] Y. Jia, P. Xiao, H. He, J. Yao, F. Liu, Z. Wang, Y. Li, Photoelectrochemical properties of polypyrrole/TiO₂ nanotube arrays nanocomposite under visible light, *Appl. Surf. Sci.* 258 (2012) 6627–

6631, <https://doi.org/10.1016/j.apsusc.2012.03.092>

- [11] N. Plylahan, S. Maria, T. N. T. Phan, M. Letiche, H. Martinez, C. Courreges, P. Knauth, T. Djenizian, Enhanced electrochemical performance of Lithium-ion batteries by conformal coating of polymer electrolyte, *Nanoscale Res. Lett.* 9 (2014) 544, <https://doi.org/10.1186/1556-276X-9-544>
- [12] N. A. Kyeremateng, F. Dumur, P. Knauth, B. Pecquenard, Electrodeposited copolymer electrolyte into nanostructured titania electrodes for 3D Li-ion microbatteries, *Comptes Rendus Chimie*, 16 (2013) 80–88, <https://doi.org/10.1016/j.crci.2012.05.002>
- [13] N. Plylahan, N. A. Kyeremateng, M. Eyraud, F. Dumur, H. Martinez, L. Santinacci, P. Knauth, T. Djenizian, Highly conformal electrodeposition of copolymer electrolytes into titania nanotubes for 3D Li-ion batteries, *Nanoscale Res. Lett.* 7 (2012) 349, <https://doi.org/10.1186/1556-276X-7-349>
- [14] Z. Wang, X. Peng, C. Huang, X. Chen, W. Dai, X. Fu, CO gas sensitivity and its oxidation over TiO₂ modified by PANI under UV irradiation at room temperature, *Appl. Catal. B* 219 (2017) 379–390, <https://doi.org/10.1016/j.apcatb.2017.07.080>
- [15] A. Victorious, A. Clifford, S. Saha, I. Zhitomirsky, L. Soleymani, Integrating TiO₂ nanoparticles within a catecholic polymeric network enhances the photoelectrochemical response of biosensors, *J. Phys. Chem. C* 123 (2019) 16186–16193, <https://doi.org/10.1021/acs.jpcc.9b02740>
- [16] T. Ma, R. Kojima, D. Tadaki, J. Zhang, Y. Kimura, M. Niwano, Fabrication of polymer/TiO₂-nanotube-based hybrid structures using a solvent-vapor-assisted coating method, *Mater. Res. Express* 1 (2014) 045048, <https://doi.org/10.1088/2053-1591/1/4/045048>
- [17] E. Baran, B. Yazıcı, Preparation and characterization of poly (3-hexylthiophene) sensitized Ag doped TiO₂ nanotubes and its carrier density under solar light illumination, *Thin Solid Films*, 627 (2017) 82–93, <https://doi.org/10.1016/j.tsf.2017.02.051>
- [18] N. Imaz, O. Zubillaga, G. Imbuluzqueta, F. Cano, anodic ordered titania nanostructures and in-situ electropolymerized poly-3-methylthiophene films for hybrid photovoltaic solar cells, *Energy Procedia*, 31 (2012) 124–135, <https://doi.org/10.1016/j.egypro.2012.11.174>
- [19] M. Bustamante-Torres, D. Romero-Fierro, J. Estrella-Nuñez, B. Arcentales-Vera, E. Chichande-Proañó, E. Bucio, Polymeric Composite of Magnetite Iron Oxide Nanoparticles and Their Application in

Biomedicine: A Review, *Polymers*, 14 (2022) Art. no. 4, <https://doi.org/10.3390/polym14040752>

[20] F. Garavand, I. Cacciotti, N. Vahedikia, A. Rehman, O. Tarhan, S. Akbari-Alavijeh, R. Shaddel, A. Rashidinejad, M. Nejatian, S. Jafarzadeh, M. Azizi-Lalabadi, S. Khoshnoudi-Nia, S. M. Jafari, A comprehensive review on the nanocomposites loaded with chitosan nanoparticles for food packaging, *Crit. Rev. Food Sci. Nutr.* 62 (2022) 1383–1416, <https://doi.org/10.1080/10408398.2020.1843133>

[21] S. N. Moya Betancourt, J. G. Uranga, A. V. Juarez, C. I. Cámara, G. Pozo López, J. S. Riva, Effect of bare and polymeric-modified magnetic nanoparticles on the drug ion transfer across liquid/liquid interfaces, *J. Electroanal. Chem.* 919 (2022) 116502, <https://doi.org/10.1016/j.jelechem.2022.116502>

[22] X. Yuan, D. Dragoë, P. Beaunier, L. Ramos; M.G. Méndez Medrano, H. Remita, Modified Polypyrrole Nanostructures with Nanoparticles (Pt, Ni) as Photocatalysts for H₂ Generation. *J. Mater. Chem. A*, 8, 268-277 (2020) <https://doi.org/10.1039/C9TA11088G>

[23] X. Yuan, C. Wang, D. Dragoë, P. Beaunier, C. Colbeau, H. Remita Highly promoted photocatalytic hydrogen generation by multiple electron transfer pathways *Applied Catalysis B: Environmental*, 281, 2021, 119457, <https://doi.org/10.1016/j.apcatb.2020.119457>

[24] D. Kowalski, P. Schmuki, Polypyrrole self-organized nanopore arrays formed by controlled electropolymerization in TiO₂ nanotube template, *Chem. Commun.* 46 (2010) 8585, <https://doi.org/10.1039/c0cc03184d>

[25] J. Cai, J. Huang, M. Ge, J. Iocozzia, Z. Lin, K. Q. Zhang, Y. Lai, Immobilization of Pt nanoparticles via rapid and reusable electropolymerization of dopamine on TiO₂ nanotube arrays for reversible SERS substrates and nonenzymatic glucose sensors, *Small*, 13 (2017) 1604240, <https://doi.org/10.1002/smll.201604240>

[26] N. Plylahan, M. Letiche, M. K. S. Barr, B. Ellis, S. Maria, T. N. T. Phan, E. Bloch, P. Knauth, T. Djenizian, High energy and power density TiO₂ nanotube electrodes for single and complete lithium-ion batteries, *J. Power Sources* 273 (2015) 1182–1188, <https://doi.org/10.1016/j.jpowsour.2014.09.152>

[27] R. B. Ambade, S. B. Ambade, N. K. Shrestha, Y. C. Nah, S. H. Han, W. Lee, S. H. Lee, Polythiophene infiltrated TiO₂ nanotubes as high-performance supercapacitor electrodes, *Chem. Commun.*

49 (2013) 2308, <https://doi.org/10.1039/c3cc00065f>

[28] N. A. Kyeremateng, F. Dumur, P. Knauth, B. Pecquenard, T. Djenizian, Electropolymerization of copolymer electrolyte into titania nanotube electrodes for high-performance 3D microbatteries,

Electrochem. Commun. 13 (2011) 894–897, <https://doi.org/10.1016/j.elecom.2011.03.026>

[29] J. Duan, H. Hou, X. Liu, Q. Liao, S. Liu, Y. Yao, Sulfonated poly(phenylene oxide)/Ti³⁺/TiO₂ nanotube arrays membrane/electrode with high performances for lithium ion battery, *Ionics*, 23 (2009)

3037–3044, <https://doi.org/10.1007/s11581-017-2094-x>

[30] R. B. Ambade, S. B. Ambade, N. K. Shrestha, R. R. Salunkhe, W. Lee, S. S. Bagde, J. H. Kim, F. J. Stadler, Y. Yamauchi, S. H. Lee, Controlled growth of polythiophene nanofibers in TiO₂ nanotube arrays for supercapacitor applications, *J. Mater. Chem. A* 5 (2017) 172–180, <https://doi.org/10.1039/c6ta08038c>

[31] M. Nischk, P. Mazierski, Z. Wei, K. Siuzdak, N. A. Kouame, E. Kowalska, H. Remita, A. Zaleska-Medynska, Enhanced photocatalytic, electrochemical and photoelectrochemical properties of TiO₂ nanotubes arrays modified with Cu, AgCu and Bi nanoparticles obtained via radiolytic reduction, *Appl. Surf. Sci.* 387 (2016) 89–102, <https://doi.org/10.1016/j.apsusc.2016.06.066>

[32] J. Belloni, M. Mostafavi, H. Remita, J.L.Marignier, M.O.Delcourt Radiation-induced synthesis of mono- and multimetallic clusters and nanocolloids *New.J.Chem.*, 22, 1239-1255, (1998)

<https://doi.org/10.1039/A801445K>

[33] E. Kowalska, H. Remita, C. Colbeau-Justin, J. Hupka, J. Belloni, Modification of titanium dioxide with platinum ions and clusters: Application in photocatalysis, *Phys. Chem. C.*, 112:1124-1131 (2008), <https://doi.org/10.1021/jp077466p>

[34] M. Nischk, P. Mazierski, M. Gazda, A. Zaleska, Ordered TiO₂ nanotubes: The effect of preparation parameters on the photocatalytic activity in air purification process, *Appl. Catal. B* 144 (2014) 674–685,

<https://doi.org/10.1016/j.apcatb.2013.07.041>

[35] M. C. Nevárez-Martínez, M. P. Kobylanski, P. Mazierski, J. Wolkievicz, G. Trykowski, A. Malankowska, M. Kozak, P. J. Espinoza-Montero, A. Zaleska-Medynska, Self-organized TiO₂-MnO₂ nanotube arrays for efficient photocatalytic degradation of toluene, *Molecules*, 22 (2017) 564,

<https://doi.org/10.3390/molecules22040564>

- [36] M. Kozak, P. Mazierski, J. Zebrowska, M. Kobylanski, T. Klimczuk, W. Lisowski, G. Tykowski, G. Nowaczyk, A. Zaleska-Medynska, Electrochemically obtained TiO₂/Cu_xO_y nanotube arrays presenting a photocatalytic response in processes of pollutants degradation and bacteria inactivation in aqueous phase, *Catalysts*, 8 (2018) Art. no. 6, <https://doi.org/10.3390/catal8060237>
- [37] M. P. Kobylański, P. Mazierski, A. Malankowska, M. Kozak, M. Diak, M. J. Winiarski, T. Kimczuk, W. Lisowski, G. Nowaczyk, A. Zaleska-Medynska, TiO₂-Co_xO_y composite nanotube arrays via one step electrochemical anodization for visible light-induced photocatalytic reaction, *Surf. Interfaces* 12 (2018) 179–189, <https://doi.org/10.1016/j.surfin.2018.06.001>
- [38] X. Wang, A. K. K. Kyaw, C. Yin, F. Wang, Q. Zhu, T. Tang, P. I. Yee, J. Xu, Enhancement of thermoelectric performance of PEDOT:PSS films by post-treatment with a superacid, *RSC Adv.* 8 (2018) 18334–18340, <https://doi.org/10.1039/C8RA02058B>
- [35] L. Feng, X. Sun, S. Yao, C. Liu, W. Xing, J. Zhang, 3 - Electrocatalysts and Catalyst Layers for Oxygen Reduction Reaction, in: W. Xing, G. Yin, and J. Zhang, *Rotating Electrode Methods and Oxygen Reduction Electrocatalysts*, Eds. Amsterdam: Elsevier, 2014, pp. 67–132, <https://doi.org/10.1016/B978-0-444-63278-4.00003-3>
- [39] G. Greczynski, L. Hultman, X-ray photoelectron spectroscopy: Towards reliable binding energy referencing, *Prog. Mater. Sci.* 107 (2020) 100591, <https://doi.org/10.1016/j.pmatsci.2019.100591>
- [40] A. Pasha, A. S. Roy, M. V. Murugendrappa, O. A. Al-Hartomy, S. Khasim, Conductivity and dielectric properties of PEDOT-PSS doped DMSO nano composite thin films, *J Mater Sci: Mater Electron*, 27 (2016) 8332–8339, <https://doi.org/10.1007/s10854-016-4842-5>
- [41] E. Susanti, P. Wulandari, Herman, Effect of localized surface plasmon resonance from incorporated gold nanoparticles in PEDOT:PSS hole transport layer for hybrid solar cell applications, *J. Phys.: Conf. Ser.*, 1080 (2018) 012010, <https://doi.org/10.1088/1742-6596/1080/1/012010>
- [42] X. Niu, L. Sun, X. Zhang, Y. Sun, J. Wang, Fabrication and antibacterial properties of cefuroxime-loaded TiO₂ nanotubes, *Appl. Microbiol. Biotechnol.* 104 (2020) 2947–2955, <https://doi.org/10.1007/s00253-020-10446-w>
- [43] Th. Braunschweig, U. Roland, H. Winkler, Electrical conductivity study of hydrogen spillover on

TiO₂, in *Studies in Surface Science and Catalysis*, vol. 77, Elsevier, 1993, pp. 183–188,

[https://doi.org/10.1016/S0167-2991\(08\)63172-9](https://doi.org/10.1016/S0167-2991(08)63172-9)

[44] P. Mazierski, A. Malankowska, M. Kobylanski, M. Diak, M. Kozak, M. J. Winiarski, T. Kimczuk, W. Lisowski, G. Nowaczyk, A. Zaleska-Medynska, Photocatalytically active TiO₂/Ag₂O nanotube arrays interlaced with silver nanoparticles obtained from the one-step anodic oxidation of Ti–Ag alloys, *ACS Catal.* 7 (2017) 2753–2764, <https://doi.org/10.1021/acscatal.7b00056>

[45] K. C. Sun, Y. C. Chen, M. Y. Kuo, H. W. Wang, Y. F. Lu, J. C. Chung, Y. C. Liu, Y. Z. Zeng, Synthesis and characterization of highly ordered TiO₂ nanotube arrays for hydrogen generation via water splitting, *Mater. Chem. Phys.* 129 (2011) 35–39, <https://doi.org/10.1016/j.matchemphys.2011.03.081>

[46] R. P. Antony, T. Mathews, C. Ramesh, N. Murugesan, A. Dasgupta, S. Dhara, S. Dash, A. K. Tyagi, Efficient photocatalytic hydrogen generation by Pt modified TiO₂ nanotubes fabricated by rapid breakdown anodization, *Int. J. Hydrog. Energy* 37 (2012) 8268–8276, <https://doi.org/10.1016/j.ijhydene.2012.02.089>

[47] D. D'Elia, C. Beauger, J. F. Hochepped, A. Rigacci, M. H. Berger, N. Keller, V. Keller-Spitzer, Y. Suzuki, J. C. Valmalette, M. Benabdesselam, P. Achard, Impact of three different TiO₂ morphologies on hydrogen evolution by methanol assisted water splitting: Nanoparticles, nanotubes and aerogels, *Int. J. Hydrog. Energy* 36 (2011) 14360–14373, <https://doi.org/10.1016/j.ijhydene.2011.08.007>

[48] S. Xu, A. J. Du, J. Liu, J. Ng, D. D. Sun, Highly efficient CuO incorporated TiO₂ nanotube photocatalyst for hydrogen production from water, *Int. J. Hydrog. Energy* 36 (2011) 6560–6568, <https://doi.org/10.1016/j.ijhydene.2011.02.103>